Molecular Therapy
Methods & Clinical Development
Original Article

rAAVrh74.MCK.*GALGT2* Demonstrates Safety and Widespread Muscle Glycosylation after Intravenous Delivery in C57BL/6J Mice

Deborah A. Zygmunt,[1,6] Rui Xu,[1,6,7] Ying Jia,[1] Anna Ashbrook,[1,2] Chelsea Menke,[2] Guohong Shao,[1] Jung Hae Yoon,[1,8] Sonia Hamilton,[1] Harshan Pisharath,[3] Brad Bolon,[4] and Paul T. Martin[1,5]

[1]Center for Gene Therapy, Abigail Wexner Research Institute at Nationwide Children's Hospital, 700 Children's Drive, Columbus, OH, USA; [2]Animal Resources Core, Abigail Wexner Research Institute at Nationwide Children's Hospital, Columbus, OH, USA; [3]Animal Resource Center and Department of Pathology, St. Jude Children's Research Hospital, Memphis, TN, USA; [4]GEMpath, Longmont, CO, USA; [5]Department of Pediatrics, The Ohio State University, Columbus, OH, USA

rAAVrh74.MCK.*GALGT2* is a surrogate gene therapy that inhibits muscular dystrophy in multiple animal models. Here, we report on a dose-response study of functional muscle *GALGT2* expression as well as toxicity and biodistribution studies after systemic intravenous (i.v.) delivery of rAAVrh74.MCK.*GALGT2*. A dose of 4.3 × 10^{14}vg/kg (measured with linear DNA standard) resulted in *GALGT2*-induced glycosylation in the majority of skeletal myofibers throughout the body and in almost all cardiomyocytes, while several lower doses also showed significant muscle glycosylation. No adverse clinical signs or treatment-dependent changes in tissue or organ pathology were noted at 1 or 3 months post-treatment. Blood cell and serum enzyme chemistry measures in treated mice were all within the normal range except for alkaline phosphatase (ALP) activity, which was elevated in serum but not in tissues. Some anti-rAAVrh74 capsid T cell responses were noted at 4 weeks post-treatment, but all such responses were not present at 12 weeks. Using intramuscular delivery, *GALGT2*-induced muscle glycosylation was increased in *Cmah*-deficient mice, which have a humanized sialoglycome, relative to wild-type mice, suggesting that use of mice may underestimate *GALGT2* activity in human muscle. These data demonstrate safety and high transduction of muscles throughout the body plan with i.v. delivery of rAAVrh74.MCK.*GALGT2*.

INTRODUCTION

rAAVrh74.MCK.*GALGT2* is a muscle-specific gene therapy designed to overexpress the human *GALGT2* transgene (also called *B4GALNT2*) in heart and skeletal muscle, where it acts as a β1,4 N-acetylgalactosaminyltransferase to glycosylate α dystroglycan.[1–9] In adult skeletal muscle, expression of *GALGT2* is confined to the neuromuscular and myotendinous junction, and its expression is also very low in the heart.[10–12] The confinement of *GALGT2* to specialized subdomains of the skeletal myofiber, which contains hundreds of nuclei, is similar to that of other synaptic dystroglycan-binding proteins, including utrophin, plectin 1f, laminin α4, laminin α5, and agrin.[13–18] When overexpressed in skeletal muscle, *GALGT2* induces glycosylation of α dystroglycan and increases the ectopic expression of its normally synaptic binding partners, many of which can inhibit the development of muscular dystrophy when overexpressed.[1,12,19,20] *GALGT2* overexpression, including that induced by rAAVrh74.MCK.*GALGT2*, has been shown to inhibit the development of disease in four different forms of muscular dystrophy: the *mdx* mouse model of Duchenne muscular dystrophy (DMD),[1,3,5,9] the dy^W mouse model of congenital muscular dystrophy 1A (MDC1A),[2] the $Sgca^{-/-}$ mouse model of limb girdle muscular dystrophy 2D (LGMD2D),[4] and the $FKRP^{P448L}$ mouse model of limb girdle muscular dystrophy 2I (LGMD2I).[7] *GALGT2* overexpression can prevent eccentric contraction-induced muscle damage not only in dystrophic *mdx* mouse muscles but also in wild-type mouse skeletal muscles, where it can induce therapeutic protein overexpression as well.[5,20] We have also recently shown that *GALGT2* overexpression in *mdx* mouse heart can prevent the loss of cardiac function as the mice age.[9] Such data have encouraged the development of a pre-clinical, and now a clinical, program to use rAAVrh74.MCK.*GALGT2* to treat patients with DMD and other forms of muscular dystrophy.

Pre-clinical efficacy, biodistribution, and toxicity studies, including investigational new drug (IND)-enabling good laboratory practice (GLP)-compliant studies, have been done to support clinical trials of rAAVrh74.MCK.*GALGT2* using intramuscular (IM) injection and using intra-arterial delivery with an isolated limb infusion (ILI) protocol.[5,8] These are logical steps to demonstrate safety prior to a first-in-human gene therapy trial using systemic intravenous (i.v.) delivery. Here, we have performed pre-clinical studies that support i.v. delivery

Received 22 July 2019; accepted 15 October 2019;
https://doi.org/10.1016/j.omtm.2019.10.005.

[6]These authors contributed equally to this work.

[7]Present address: Pfizer, Inc., Morrisville, NC, USA

[8]Present address: University of Florida, Gainesville, FL, USA

Correspondence: Paul T. Martin, Center for Gene Therapy, Abigail Wexner Research Institute at Nationwide Children's Hospital, 700 Children's Drive, Columbus, OH, USA.
E-mail: paul.martin@nationwidechildrens.org

of rAAVrh74.MCK.*GALGT2* to all skeletal muscles and the heart. These studies include dose-response studies to demonstrate muscle cell glycosylation and adeno-associated virus (AAV) biodistribution, and toxicity studies at very high doses to demonstrate safety. While clinical ILI studies at lower doses in isolated limbs are ongoing (NCT: 03333590), the studies presented here are the first to test the much higher doses required for systemic i.v. delivery of *GALGT2* to all muscle tissues. Such studies are needed to support an amendment to the IND to allow for higher dose systemic i.v. delivery.

RESULTS

GALGT2 Overexpression Induces Glycosylation of Skeletal and Cardiac Muscles in Response to Different Intravenous Doses of rAAVrh74.MCK.GALGT2

We treated young adult (8-week-old) male C57BL/6J wild-type mice with rAAVrh74.MCK.*GALGT2* by injecting doses intravenously (i.v.) in the tail vein. Only male mice were used in all of our studies, as these studies pertain to the use of *GALGT2* gene therapy in patients with DMD, an X-linked disease occurring almost entirely in boys.[21,22] To determine the dose of AAV used, we compared AAV titers using a linear and a supercoiled DNA standard, finding that titers with the linear standard were, on average, 2.8 times lower than the titers calculated using the supercoiled standard. For this study, we used the linear standard to calculate dose and injected the mice with 4.3×10^{14} vector genomes per kilogram (vg/kg), 1.4×10^{14} vg/kg, 4.8×10^{13} vg/kg, 1.6×10^{13} vg/kg, or 5.2×10^{12} vg/kg rAAVrh74.MCK.*GALGT2*. A linear dose of 4.3×10^{14} vg/kg, then, would be equivalent to a dose of 1.2×10^{15} vg/kg using a supercoiled standard, which was the supercoiled standard dose we used in a previous study to demonstrate the prevention of loss of cardiac function in *mdx* mice.[9] Mice were analyzed for cytotoxic T cell (CT) glycan expression at 1 and 3 months post-treatment using *Wisteria floribunda* agglutinin (WFA) lectin staining to identify the terminal β1,4GalNAc linkage made by *GALGT2*. Laminin α2 co-staining was done to mark the extracellular matrix (ECM) surrounding each skeletal myofiber. 2 mice per group were used for this assessment to limit animal use, as the experiment involved 5 different doses and two different time points.

We analyzed frozen sections from heart and from various skeletal muscles, including trapezius, intercostal, triceps brachii, biceps brachii, diaphragm, gluteus maximus, quadriceps femoris, gastrocnemius, and tibialis anterior. For muscles with distinct segments (e.g., medial and lateral heads of the gastrocnemius), we analyzed all regions together. Examples of muscle sections stained at different doses are shown for heart (Figure 1), diaphragm (Figure 2), and tibialis anterior (Figure S1). Examples of staining for diaphragm, biceps brachii, tibialis anterior, gastrocnemius, gluteus maximus, and intercostal muscles at the dose of 4.3×10^{14} vg/kg are shown in Figure 3. At 1 month post-treatment with 4.3×10^{14} vg/kg rAAVrh74.MCK.*GALGT2*, WFA stained high numbers of myofibers in certain regions of all heart and skeletal muscles. We next quantified the percentage of WFA cardiomyocytes or skeletal myofibers that were positive relative to the number of laminin-α2-stained muscle fibers (Figures 4A and 4B) and also quantified AAV vector biodistribution (Figures 4C and 4D) and GALGT2 mRNA induction (Figure 4E). *GALGT2*-induced glycosylation was very high in the heart at 1 month post-treatment when the highest dose was used (95% of all cardiomyocytes), while skeletal muscles showed a lower overall extent of glycosylation (Figure 4A). Skeletal muscle glycosylation at the highest dose ranged from 40%–50% in the diaphragm, biceps, and intercostal to 15%–20% in the trapezius, triceps, and quadriceps femoris, with the gastrocnemius, tibialis anterior, and gluteus maximus showing an intermediate level of transduction (20%–30%; Figure 4A). The extent of glycosylation in heart and in skeletal muscles, however, was increased when muscles were analyzed at 3 months post-treatment (Figure 4B). At this time point, all skeletal muscles now showed 30%–50% positive staining for WFA at the highest dose (4.3×10^{14}vg/kg) and showed increased glycosylation at the dose of 1.4×10^{14} vg/kg relative to expression at 1 month. Staining exceeded 20% of all myofibers at 3 months for the dose of 1.4×10^{14} vg/kg in the diaphragm, intercostal, biceps brachii, gastrocnemius, tibialis anterior, quadriceps femoris, gluteus maxiumus, and trapezius muscle, a level of transduction previously shown to elicit significant protection against muscle membrane damage.[5] In addition, all skeletal muscles tested and heart showed increased glycosylation at the dose of 4.8×10^{13} vg/kg at 3 months relative to 1 month. Thus, the kinetics of glycosylation induced by *GALGT2* was slow, showing increased numbers of muscle cells stained with WFA at 3 months relative to 1 month of treatment.

Biodistribution studies of AAV vector genomes (vgs) in skeletal muscle at 1 (Figure 4C) and 3 (Figure 4D) months post-treatment showed a clear dose-response relationship in all skeletal muscles, increasing from 10^3 vg/μg genomic DNA at the dose of 5.2×10^{12} vg/kg to greater than 10^5 vg/μg at the dose of 4.3×10^{14} vg/kg. We performed *GALGT2* gene expression studies in diaphragm, gastrocnemius, and heart at 1 and 3 months post-treatment (Figure 4E). These measures were normalized to endogenous mouse *Galgt2* expression in mock-treated muscles receiving only buffer. It is important to remember that endogenous mouse *Galgt2* expression is confined to only neuromuscular and myotendinous junctions in adult skeletal muscles;[10,11] therefore, expression of endogenous *Galgt2* mRNA is very low. This makes the levels of induction accordingly quite high, as shown previously.[7,20] Again, there was a clear dose-response relationship to induction of *GALGT2* mRNA expression in all instances, with a maximal fold induction in diaphragm, gastrocnemius, and heart of 2,000-fold or more at 4.3×10^{14} vg/kg. In almost all instances, gene expression at various doses was increased at 3 months versus 1 month, mirroring what was seen for vector biodistribution (Figures 4C and 4D). Last, we compared fold induction of *GALGT2* mRNA to vector genomes present for all doses tested in heart, diaphragm and gastrocnemius (Figure 4F). This showed a clear correlation between the two measures ($R^2 = 0.91$).

GALGT2-Induced Muscle Glycosylation and GALGT2 Glycan Binding Are Increased for Human Sialic Acid Glycoforms

As GALGT2 requires a sialylated glycan as a substrate for enzymatic activity,[23] we wanted to understand whether the deletion of *Cmah*, which modifies CMP-N-acetyl-neuraminic acid (CMP-Neu5Ac) to make CMP-N-glycolyl-neuraminic acid (CMP-Neu5Gc),[24,25] would

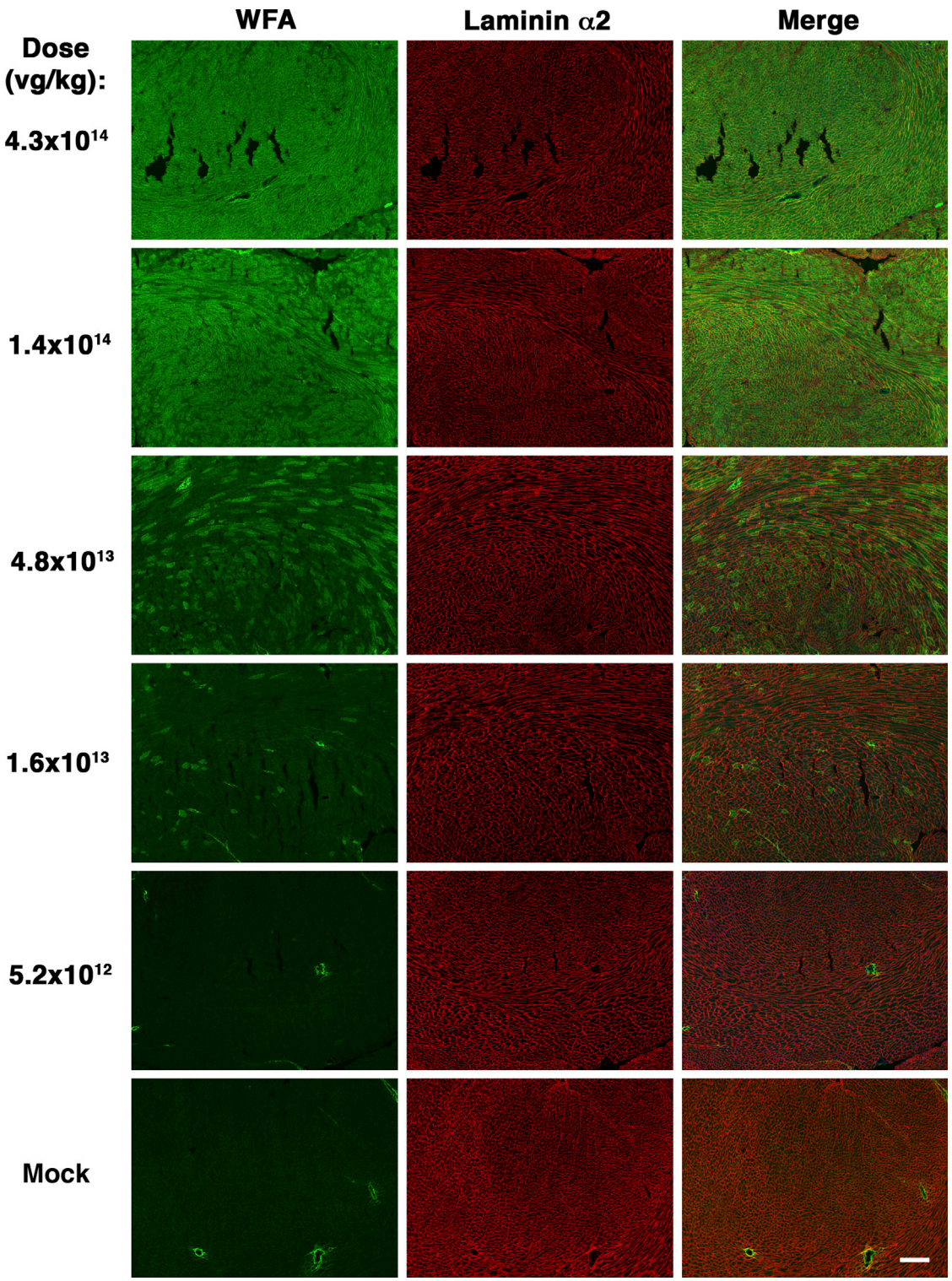

Figure 1. *GALGT2*-Induced Glycosylation in the Heart in Response to Different Doses of rAAVrh74.MCK.*GALGT2*

Heart muscles from wild-type C57BL/6J mice treated with different i.v. doses of rAAVrh74.MCK.*GALGT2* for 1 month were stained with *Wisteria floribunda* agglutinin (WFA, green) to identify cardiomyocytes overexpressing *GALGT2* and with laminin α2 (red) to identify all muscle cells. Merged image is shown at right with overlap in orange-yellow. Scale bar, 400 μm.

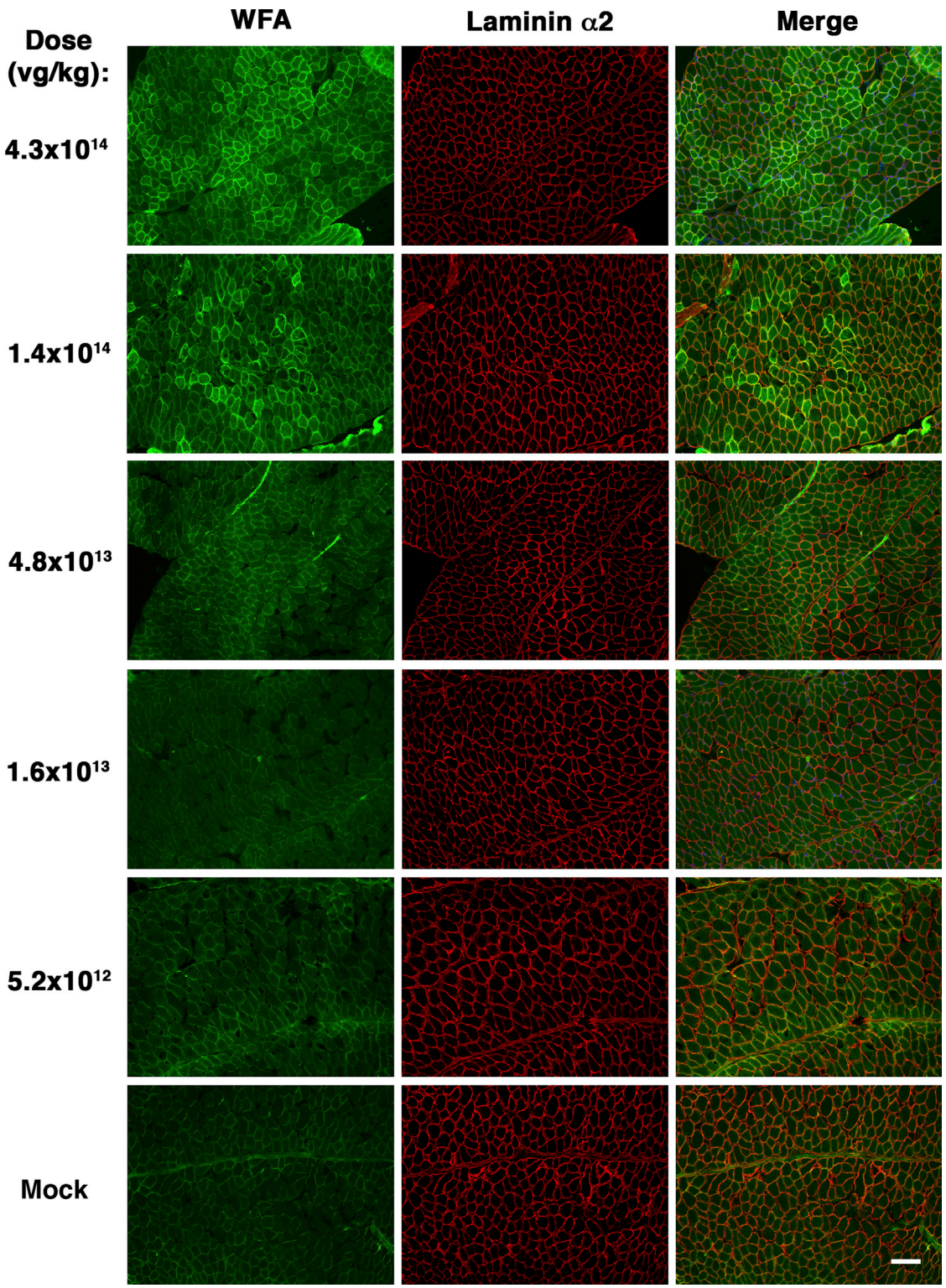

Figure 2. *GALGT2*-Induced Glycosylation in the Diaphragm in Response to Different Doses of rAAVrh74.MCK.*GALGT2*

Diaphragm muscles from wild-type C57BL/6J mice treated with different i.v. doses of rAAVrh74.MCK.*GALGT2* for 1 month were stained with *Wisteria floribunda* agglutinin (WFA, green) to identify skeletal myofibers overexpressing *GALGT2* and with laminin α2 (red) to identify all muscle cells. Merged image is shown at right with overlap in orange-yellow. Scale bar, 100 μm.

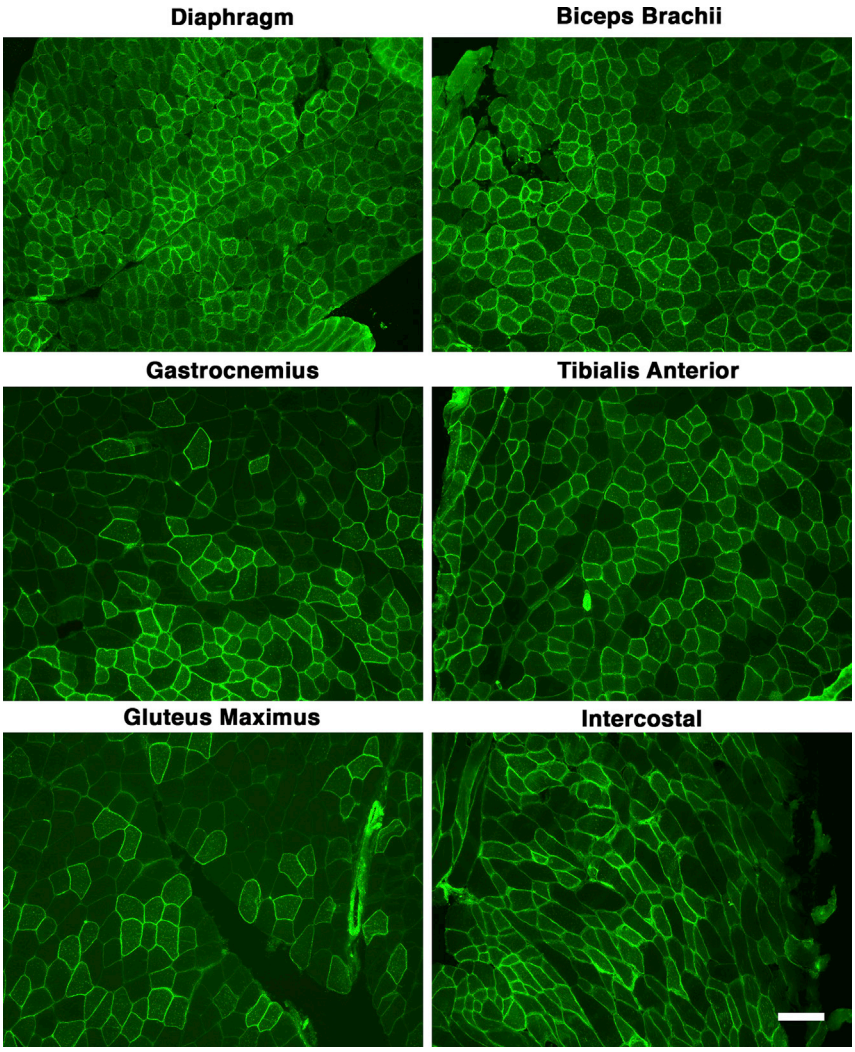

Figure 3. Examples of Skeletal Muscle Glycosylation after a 4.3 × 10^{14} vg/kg i.v. Dose of rAAVrh74.MCK.*GALGT2*

Different skeletal muscles were analyzed from wild-type C57BL/6J mice treated with i.v. doses (4.3 × 10^{14} vg/kg) of rAAVrh74.MCK.*GALGT2* for 1 month. Muscle sections were stained with *Wisteria floribunda* agglutinin (WFA, green) to identify skeletal myofibers overexpressing *GALGT2*. Scale bar, 100 μm.

alter *GALGT2*-induced glycosylation in skeletal muscle. The *Cmah*$^{-/-}$ mice used here were crossed onto a pure C57BL/6J background (>15 generations), making wild-type C57BL/6J mice an otherwise isogenic control. Mice express a functional *Cmah* gene, as do almost all other living mammals, and this leads to the biosynthesis of sialic-acid-containing glycans with either N-glycolyl-neuraminic acid (Neu5Gc) or N-acetyl-neuraminic acid (Neu5Ac) as their form of sialic acid, about a 50:50 mix in skeletal muscle.[25,26] Humans, by contrast, lack a functional *CMAH* gene and, therefore, make Neu5Ac but not Neu5Gc, a genetic change that occurred approximately 2–3 million years ago after early humans evolved from the great apes.[27] As such, human *GALGT2*[28] may bind Neu5Ac, a human sialic acid, better than Neu5Gc, a non-human sialic acid, much as has been shown for other human sialic-acid-binding proteins.[29,30]

To assess this, we generated an IM dose-response curve in the tibialis anterior muscle of young adult (8-week-old) C57BL/6J and *Cmah*$^{-/-}$ mice (Figure 5A). We compared rAAVrh74.MCK.*GALGT2* and rAAVrh74.MHCK7.*GALGT2* IM injection doses of 3.5 × 10^{9} vg, 3.5 × 10^{10} vg, and 1.8 × 10^{11} vg, analyzing muscle expression 12 weeks after injection. We used 10 mice per group here to reduce the variability that occurs with IM injection and to power the analysis so as to see significant differences even with relatively modest changes. At the dose of 3.5 × 10^{9}, we saw a significant increase in *GALGT2*-dependent glycosylation of myofibers in *Cmah*$^{-/-}$ mice compared to wild-type using either the MCK or the MHCK7 promoter. This did not correlate with any significant change in the number of vgs present in the different muscle groups (data not shown) or in *GALGT2* gene expression in wild-type versus *Cmah*$^{-/-}$ groups (Figure 5B). The MHCK7 promoter induced more *GALGT2* gene expression in skeletal muscle than the MCK promoter did (Figures 5A and 5B), consistent with previous studies.[31]

We next compared the binding of recombinant mouse Galgt2 or human GALGT2 protein to sialyl-N-acetyllactosamine (SNL), a known glycan substrate for GALGT2, in its Neu5Ac or Neu5Gc glycoform (Figure 5C). Here, we performed only 2 experiments per condition, as biotinylated glycans were in limited supply. We also compared the binding of these proteins to N-acetyllactosamine (Galβ1,4GlcNAcβ-, NL), Galα1,3Galβ1,4GlcNAcβ- (GalNL), and Galβ1,4GlcNAcβ1,3Galβ1,4GlcNAcβ- (diNL), all of which lack sialic acid, as controls, as well as the CT glycan (GalNAcβ1,4[Neu5Acα2,3]Galβ1,4GlcNAcβ-, CT), the product of GALGT2 enzymatic activity.[23,28] Both mouse and human GALGT2 showed equivalent binding to 3′SNL(5Ac), but mouse Galgt2 protein showed more than twice the level binding to 3′SNL(5Gc), while human GALGT2 bound 3′SNL(5Gc) more poorly. Thus, human GALGT2 preferentially bound the 3′SNL, a known substrate[23] when Neu5Ac was present, which is the sialic acid glycoform present in humans.[27] Both human GALGT2 and mouse Galgt2 protein bound α2,6-linked SNL (5Gc), which can also be a GALGT2 substrate,[32] but again, mouse Galgt2 bound the Neu5Gc form more than the Neu5Ac form, while human GALGT2 bound these two structures equally well. Neither human GALGT2 nor mouse Galgt2 protein showed appreciable binding to

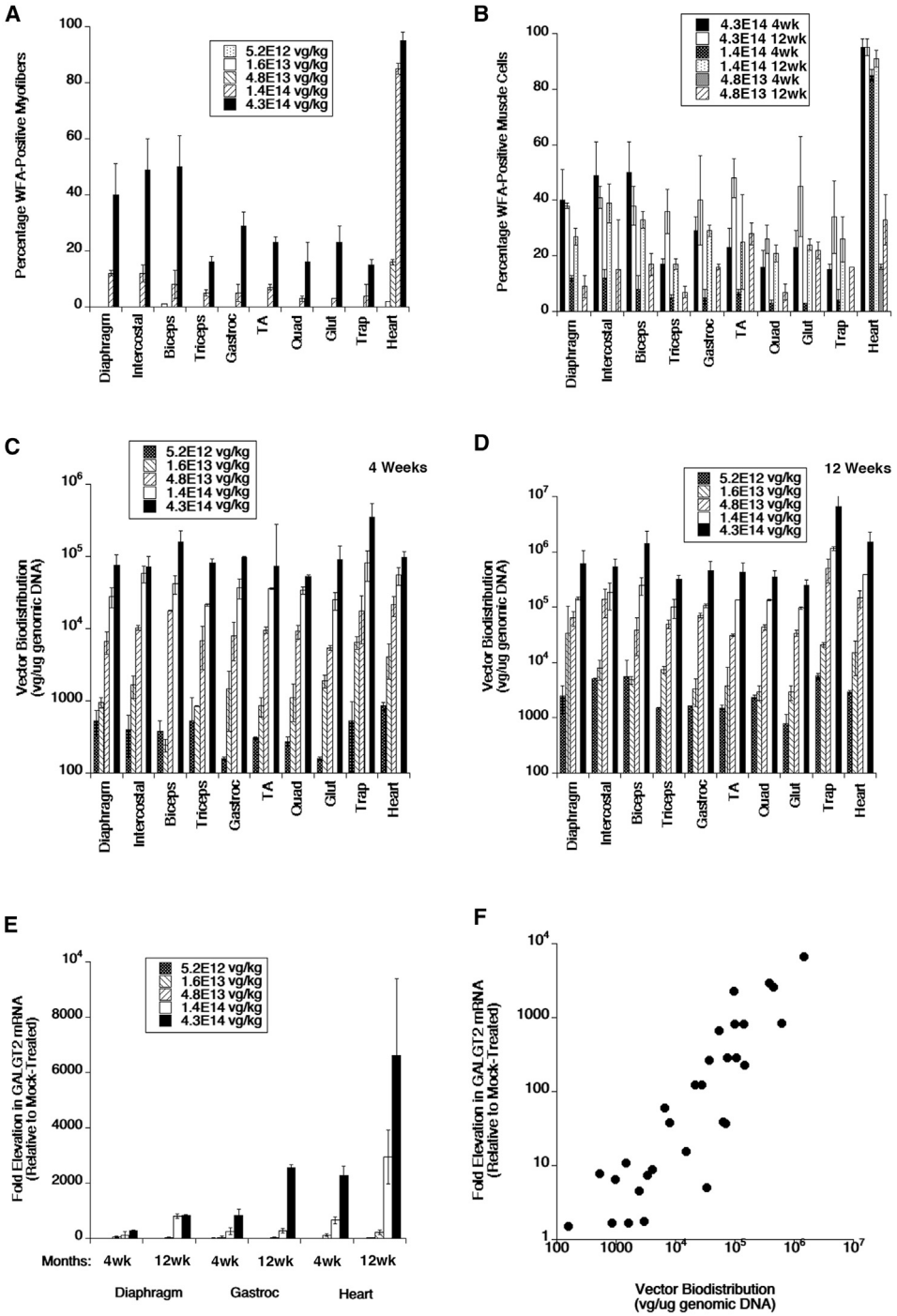

Figure 4. Quantification of *GALGT2*-Induced Glycosylation, AAV Vector Biodistribution, and *GALGT2* Gene Expression after i.v. Dosing of rAAVrh74.MCK.*GALGT2*

(A and B) Wild-type C57BL/6J mice treated with different i.v. doses of rAAVrh74.MCK.*GALGT2* were analyzed for the percentage of cardiomyocytes or skeletal myofibers overexpressing *GALGT2* as evidenced by WFA staining at 1 month (A) or 3 months (B) post-treatment. (C and D) AAV vector genomes (vgs) per microgram of genomic DNA were analyzed at 1 (C) and 3 (D) months post-treatment. (E) *GALGT2* gene expression was measured as a fold induction relative to endogenous gene expression in mock-treated animals at 1 and 3 months post-treatment. (F) AAV copy number and *GALGT2* gene expression for all doses tested in diaphragm, heart, and gastrocnemius muscles were plotted to demonstrate the relationship between AAV vgs present and *GALGT2* gene expression. Error bars represent SD for n = 2 measures per condition, with 5 measures in (A) and (B) or 3 measures in (C)–(F) averaged for each data point.

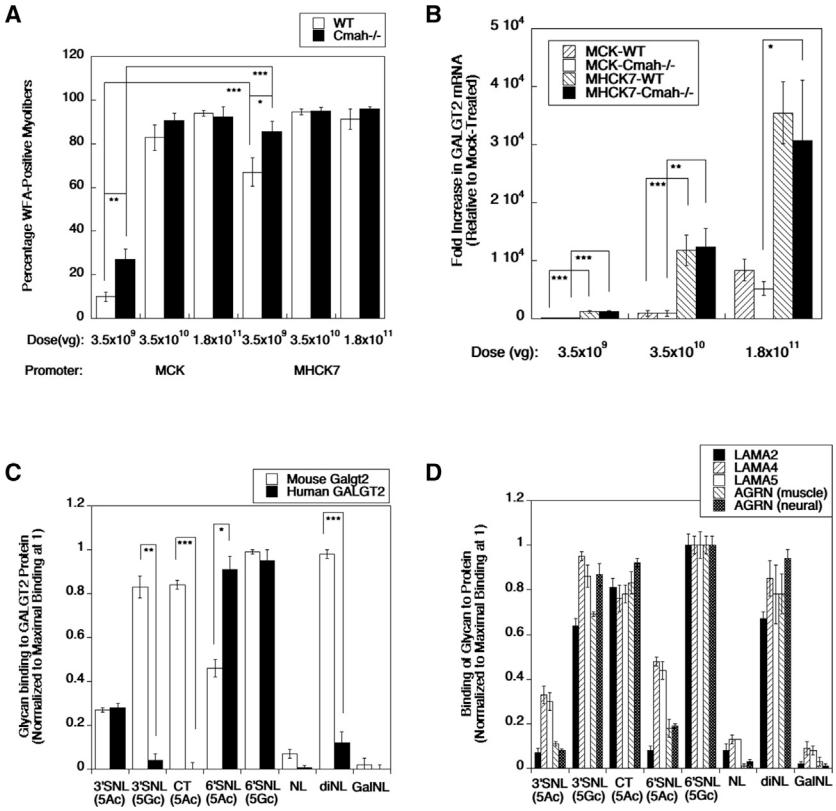

Figure 5. Role of Neu5Gc in *GALGT2*-Induced Muscle Glycosylation and Glycan Binding to GALGT2 Protein and Extracellular Matrix Proteins

Wild-type (WT) and *Cmah*$^{-/-}$ mice, which lack Neu5Gc expression, were given an intramuscular injection of rAAVrh74.*GALGT2* using the MCK or MHCK7 promoter, as indicated, in the tibialis anterior muscle. (A and B) Muscles were analyzed at 12 weeks after treatment for WFA staining of *GALGT2*-induced glycosylation (A) or *GALGT2* gene expression (B). Biotin-PAA-conjugated glycans were assayed for binding to recombinant human GALGT2 or mouse Galgt2 (C) or to recombinant G1–G5 domains of mouse laminin α2 (LAMA2), laminin α4 (LAMA4), or laminin α5 (LAMA5), or to recombinant G2-G3 domains of muscle- (z0) or nerve-specific (z8) splice forms of rat agrin (AGRN). (D) Glycans used were Neu5Acα2,3Galβ1,4GlcNAcβ-SpNH-PAA (3′SNL 5Ac), Neu5Gcα2,3Galβ1,4GlcNAcβ-SpNH-PAA (3′SNL 5Gc), Neu5Acα2,3[GalNAcβ1,4]Galβ1,4GlcNAcβ-SpNH-PAA (CT 5Ac), Neu5Acα2,6Galβ1,4GlcNAcβ-SpNH-PAA (6′SNL 5Ac), Neu5Gcα2,6Galβ1,4GlcNAcβ-SpNH-PAA (6′SNL 5Gc), Galβ1,4GlcNAcβ-SpNH-PAA (NL), Galβ1,4GlcNAcβ1,3Galβ1,4GlcNAcβ-SpNH-PAA (diNL), and Galα1,3Galβ1,4GlcNAcβ-SpNH-PAA (GalNL), where Neu5Ac is N-acetyl-neuraminic acid, Neu5Gc is N-glycolyl-neuraminic acid, Gal is galactose, GlcNAc is N-acetylglucosamine, and GalNAc is N-acetylgalactosamine. Error bars represent SEM for n = 10 animals per condition in (A) and (B). Error bars represent SD for n = 2 or per group in (C) and (D), respectively. *p < 0.05; **p < 0.01; ***p < 0.001.

NL or GalNL, as expected, as GALGT2 recognizes sialylated glycan substrates;[23,28] however, mouse Galgt2 also bound CT glycan as well as diNL, while human GALGT2 bound these glycans poorly, if at all. We also compared binding of the same glycans to recombinant forms of the G1–G5 domains of mouse laminin α2, α4, or α5 or the muscle or neural G2–G3 domains of rat agrin (Figure 5D). Binding of glycans to all of these proteins mimicked their binding pattern to mouse Galgt2.

Toxicity Study of i.v. Systemic rAAVrh74.MCK.GALGT2 Treatment of C57BL/6J Mice

We next undertook a toxicity study in collaboration with the Animal Resources Core at Nationwide Children's Hospital. 7 mice were used per condition to ensure meeting the required Food and Drug Administration (FDA) standards for gene therapy based on our previous experience. 8-week-old C57BL/6J male mice were weighed, randomized into a control vehicle cohort and a test article (rAAVrh74.MCK.*GALGT2*) cohort, and dosed at 4.3×10^{14} vg/kg (using a linear DNA standard). Each cohort was further randomized into two cohorts based on euthanasia time points, 4 or 12 weeks post-treatment, to yield four groups: group 1, vehicle only at 4 weeks post-treatment; group 2, test article at 4 weeks post-treatment; group 3, vehicle only at 12 weeks post-treatment; and group 4, test article at 12 weeks post-treatment (Table S1). Investigators performing measures were blinded to the treatment groups and to the test agent. Body weights of mice within each cohort were within 20% of the mean population at the start of the study. Because of the very large i.v. dose given, mice had to be injected 3 times, with each injection spaced 2–4 h apart. Injections were done in the lateral tail vein, with 200–250 μL of the volume used for each injection. Mice were observed daily for clinical signs, including small size, weakness, dermatitis, masses, swelling, ocular issues, wounds, malocclusions, hydrocephalus, and mortality (Table S2). No clinical signs were noted in any group, but one mouse treated with vehicle only died during a bleeding procedure at week 11. Body weights were measured weekly (Table S3). All groups showed normal gains in body weight by the time of necropsy that did not have a statistically significant difference between vehicle and treatment groups.

Hematology and Serum Chemistry Measures

Blood cell measures were within the normal range for all groups, though white blood cell counts were significantly elevated in both groups 2 and 4, relative to groups 1 and 3, respectively (Table 1). Serum chemistries showed one significant treatment-related change, elevated alkaline phosphatase (ALP) activity, both in group 2 versus 1 and group 4 versus 3 comparisons (Table 2; $p < 0.001$ for both comparisons). Both of these treatment-related elevations were outside the normal range. The only other measure outside the normal range was serum creatine kinase (CK) activity (all groups). This may have resulted from the surgery done to perform a cardiac puncture to collect blood at the time of euthanasia. Interestingly, serum CK for treatment group 4 (treated) was significantly lower than for group 3 (vehicle) ($p < 0.05$), perhaps

Table 1. Summary of Hematology Measures in Wild Type C57BL/6J Mice Treated i.v. with 4.3E+14 vg/kg rAAVrh74.MCK.*GALGT2*

	Week 4						Week 12					
	Vehicle			Test Article			Vehicle			Test Article		
Hematology Measures	Mean	SD	n	Mean	SD	n	Mean	SD	n	Mean	SD	n
Red blood cell (erythrocyte) count (10^6/μL)	9.4	0.2	6	9.3	0.6	6	9.2	0.5	6	8.6	0.7	7
White blood cell (leukocyte) count (10^3/μL)	3.2	0.4	6	4.4	1.1	6	2.7	0.8	6	4.3	0.9	7
Hematocrit (%)	55.3	1.2	6	54.1	3.6	6	49.2	2.8	6	46.0	3.0	7
Hemoglobin (g/dL)	13.5	0.6	6	13.8	0.8	6	12.8	0.7	6	12.0	1.2	7
Mean corpuscular hemoglobin (pg)	14.3	0.6	6	14.8	0.3	6	14.0	0.2	6	13.9	0.2	7
Mean corpuscular volume (fL)	58.7	1.3	6	57.9	0.6	6	53.7	2.0	6	53.4	1.9	7
Mean corpuscular hemoglobin concentration (g/dL)	24.4	1.3	6	25.5	0.5	6	26.0	1.0	6	26.1	1.2	7
Platelet count (10^3/μL)	956.5	155.0	6	699.0	325.6	6	1112.3	196.4	6	1216.3	205.1	7
Neutrophils (10^3/μL)	0.4	0.19	6	0.36	0.12	6	0.25	0.09	6	1.07	1.18	7
Lymphocytes (10^3/μL)	2.46	0.33	6	3.68	1.0	6	2.26	0.71	6	3.05	081	7
Monocytes (10^3/μL)	0.11	0.17	6	0.18	0.18	6	0.05	0.04	6	0.04	0.02	7
Eosinophils (10^3/μL)	0.16	0.12	6	0.08	0.05	6	0.06	0.04	6	0.10	0.05	7
Basophils (10^3/μL)	0.01	0.01	6	0.01	0.01	6	0.01	0.00	6	0.01	0.00	7
Reticulocytes (10^9/L)	514.8	78.1	6	627.9	129.0	6	767.3	182.2	6	974.5	413.7	7
Large unstained cells (10^3/μL)	0.04	0.02	6	0.07	0.06	6	0.04	0.02	6	0.06	0.05	7

N/A, not applicable.

indicating a prevention of muscle membrane damage by the test agent, as in previous studies.[5] All other differences, if present, involved values within the normal range for the measure in question. Because elevated ALP activity, in the absence of elevated aspartate transferase (AST) and/or alanine transferase (ALT) and/or gamma-glutamyltransferase (GGT), suggests a possible change in bone growth and/or bone pathology, we added serum calcium and phosphorus measures to the 12-week time point after seeing elevated ALP at 4 weeks. All such measures for groups 3 and 4 were within the normal range at 12 weeks.

We further investigated the elevated ALP readings in several ways. First, we measured serum ALP protein levels (Figure S2A) and serum ALP activity levels (Figure S2B) in response to the doses of rAAVrh74.MCK.*GALGT2* used in the dose-response study. There was a 2-fold elevation in serum ALP protein levels at doses of 1.6×10^{13} vg/kg and above, while significant increases in ALP activity occurred at doses of 4.6×10^{13} vg/kg and above, reaching a 10-fold elevation. WFA precipitation of serum showed no impact of removing βGalNAc-containing serum proteins on elevated ALP protein concentrations or activity levels (data not shown). We also assayed ALP activity in the muscles and organs of 3 samples each from control group 3 and treatment group 4 and found no differences in any tissue analyzed (Table S4). Thus, elevation in serum ALP levels did not arise from elevation of ALP activity in any of the tissues tested, including bone, liver, skeletal muscle, heart, kidney, lung, spleen, brain, spinal cord, pancreas, large or small intestine, stomach, testes, and lymph node.

Histopathology Evaluation

At the endpoint, mice were euthanized, and all organs were dissected, fixed, sectioned, and analyzed for organ histopathology. No visible organ pathology was evident at the time of dissection for any mouse. Bone weights and lengths were unchanged between control group 3 and treatment group 4 (Table S5). No treatment-related microscopic findings were observed in sections of heart, skeletal muscle (gastrocnemius, quadriceps femoris, diaphragm, triceps brachii), liver, spleen, kidney, pancreas, lung, lymph node, digestive tract (stomach, jejunum, colon), brain, spinal cord, testes/epididymis, or bone (femur) (Table S6). Some incidental findings were found in both the treatment and vehicle control groups. In addition, at the 12-week time point, one test-article-treated animal (1932) had one focus of minimal (>0 and <5%) myofiber degeneration (characterized by a few fibers with centrally located nuclei and small profiles) associated with minimal inflammation (chiefly, mononuclear cells) in the gastrocnemius muscle. Another mouse given test article (1929) had one minimal mononuclear cell infiltrate in the quadriceps femoris muscle. In summary, treatment with AAVrh74.MCK.*GALGT2* did not elicit significant microscopic changes in selected viscera and myofibers of multiple striated muscles at 4 and 12 weeks after i.v. administration, which indicates that this test article was well tolerated.

Biodistribution Studies

Quantitative PCR (qPCR) analysis showed the presence of rAAVrh74.MCK.*GALGT2* vector genome DNA in all tissues harvested at necropsy for both the 4- and the 12-week time points (Table 3). No positive signal was identified (<50 vg/μg genomic DNA) in any

Table 2. Summary of Clinic Chemistry Measures in Wild Type C57BL/6J Mice Treated i.v. with 4.3E+14 vg/kg rAAVrh74.MCK.*GALGT2*

	Week 4						Week 12					
	Vehicle			Test Article			Vehicle			Test Article		
Clinic Chemistry Measures	Mean	SD	n	Mean	SD	n	Mean	SD	n	Mean	SD	n
Alkaline phosphatase (U/L)	65.1	15.7	7	556.3	65.0	7	66.1	12.5	7	493.7	85.2	7
Alanine aminotransferase (U/L)	32.4	18.3	7	35.0	10.6	7	38.6	16.0	7	29.0	10.0	7
Aspartate aminotransferase (U/L)	279.9	347.3	7	298.6	279.9	7	245.9	155.4	7	113.7	79.2	7
Blood urea nitrogen (mg/dL)	29.6	1.4	7	26.3	5.0	7	35.3	5.6	7	27.9	1.1	7
Creatine kinase (U/L)	5,365.0	7,015.6	6	6,294.8	4,435.5	7	6,661.4	6,493.7	7	775.6	194.3	7
Creatinine (mg/dL)	0.3	0.1	7	0.2	0.1	7	0.2	0.0	7	0.2	0.0	7
Direct bilirubin (mg/dL)	0.0	0.1	6	0.1	0.1	6	0.0	0.0	7	0.0	0.0	7
Gamma-glutamyl transferase (U/L)	0.0	0.0	7	0.1	0.4	7	0.0	0.0	7	0.7	0.8	7
Glucose (mg/dL)	351.6	65.9	5	368.1	69.7	7	216.0	95.2	7	312.0	169.6	7
Total bilirubin (mg/dL)	0.5	0.3	7	0.5	0.1	7	0.3	0.2	7	0.2	0.0	7
Total protein (g/dL)	4.4	0.3	5	4.8	0.2	7	4.8	0.4	7	4.5	0.2	7
Calcium (mg/dL)	N/A	N/A	N/A	N/A	N/A	N/A	9.0	0.5	6	9.3	0.4	7
Phosphorus (mg/dL)	N/A	N/A	N/A	N/A	N/A	N/A	9.9	1.2	6	11.3	0.8	7

N/A, not applicable.

vehicle-treated control animals, either in cohort 1 (4 weeks) or cohort 3 (12 weeks). At 4 weeks post-treatment (cohort 2), we identified AAV vector genomes exceeding 1.7×10^5 vg/μg, or 1 vg per nucleus, in all muscles tested (calculation based on assumption of 1.7×10^5 nuclei per microgram of mouse genomic DNA). As shown by many investigators previously, liver was the most transduced tissue. Brain, large intestine, and testes, by contrast, were the only tissues at the 4-week time point transduced below 1.7×10^5 vg/μg genomic DNA. There were no statistical differences of biodistribution in the following tissues/organs between AAV-treated groups 2 (week 4) and 4 (week 12): heart, spinal cord, small intestine, lymph nodes, and testis; however, there was a significant decrease in skeletal muscles, though transduction remained near or above 1.7×10^5 vg/μg in all instances at the 12-week time point. This was in contrast to increased vgs at 12 weeks versus 4 weeks in the dose-response study (Figures 4C and 4D). Loss of vector at 12 weeks relative to 4 weeks of treatment was most apparent in blood (drop from 1.3×10^6 vg/μg to 1.45×10^3 vg/μg), liver (drop from 2.88×10^7 vg/μg to 5.52×10^6 vg/μg), large intestine (drop from 1.41×10^5 vg/μg to 2.33×10^4 vg/μg), and small intestine (drop from 7.9×10^5 vg/μg to 7.99×10^4 vg/μg). Bone showed a transduction of 1.89×10^5 vg/μg at 12 weeks post-treatment, a level equivalent to the transduction of skeletal muscle. We did not assess the extent or distribution of AAV vg integration into the host mouse genome, but previous studies have shown that such integration effects do occur, albeit infrequently.[33,34]

Immune Responses to rAAVrh74.MCK.GALGT2

Antibody titers to AAVrh74 capsid and GALGT2 protein were determined on serum samples from mice at week 4 and/or 12 weeks post-rAAV.rh74.MCK.*GALGT2* administration (Table S7). Vehicle-treated mice were also assayed. Antibody titers of <1:100 were observed in all vehicle-treated control animals at both time points for rAAVrh74 capsid protein. In test-article-treated animals, antibody titers were 1:3,200 and 1:6,400 in group 2 (4 weeks post-treatment) and were as low as 1:3,200 in one sample and as high as 1:25,600 in 3 samples in group 4 (12 weeks post-treatment). This level of antibody production would be expected to inhibit muscle transduction by AAV, as we have previously shown that serum antibody titers of 1:800 to rAAVrh74 can block muscle expression of both micro-dystrophin and *GALGT2* gene therapy when rAAVrh74 was used.[6,20] No antibody titer was measured at <1:50 to GALGT2 protein in serum from rAAVrh74.MCK.*GALGT2*-treated mice at 12 weeks. Enzyme-linked immunospot (ELISpot) assay was done on splenocytes collected at the time of necropsy (Table S8). There were no positive cell-mediated immune responses to rAAVrh.74 capsid protein in samples from vehicle-administrated groups (groups 1 and 3) at either the 4-week or the 12-week time point. At the 4-week time point, less than half (43%) of the samples from the test-article-treated group (group 2) had transient positive immune responses to AAVrh74 capsid protein peptide pools 2 and 3, but there were no immune responses to capsid protein peptide pool 1. All the samples from the test-article-treated group at the 12-week time point (group 4) had no immune responses to AAVrh74 capsid. There were no positive cell-mediated immune responses to the GALGT2 protein in either vehicle-treated groups (groups 1 and 3) or test-article-treated groups (groups 2 and 4) at either the 4-week or 12-week time point.

DISCUSSION

In developing rAAVrh74.MCK.*GALGT2* gene therapy for patients with DMD, we have adopted a stepwise approach to gene delivery that can be moved into clinical practice. This has involved moving from a single IM injection to ILI, to i.v. injection as the means of

Table 3. Summary of AAV Vector Genome (vg) Measures in Wild-Type C57BL/6J Mice Treated i.v. with 4.3E+14 vg/kg rAAVrh74.MCK.*GALGT2*

	Week 4		Week 12	
Tissues and Organs	Average	SD	Average	SD
Heart	7.79E+05	5.10E+05	5.25E+05	6.01E+05
Diaphragm	6.09E+05	1.69E+05	2.09E+05	1.82E+05
Triceps	8.69E+05	4.75E+05	1.74E+05	1.44E+05
Quadriceps	1.49E+06	1.17E+06	1.33E+05	1.01E+05
Gastrocnemius	7.21E+05	3.15E+05	1.50E+05	9.63E+04
Brain	6.29E+04	2.24E+04	3.66E+04	1.08E+04
Spinal cord cervical	7.90E+05	4.06E+05	5.55E+05	3.43E+05
Spinal cord lumbar	4.94E+05	2.49E+05	9.69E+05	8.89E+05
Lung	1.08E+06	5.69E+05	2.76E+05	1.43E+05
Stomach	3.39E+05	2.93E+05	6.95E+04	5.20E+04
Small intestine	7.90E+05	1.29E+06	7.99E+04	2.81E+04
Large intestine	1.41E+05	2.67E+04	2.33E+04	1.43E+04
Liver	2.88E+07	1.05E+07	5.52E+06	5.70E+06
Pancreas	2.51E+05	1.02E+05	1.02E+05	1.08E+05
Kidney	6.26E+05	3.69E+05	1.32E+05	7.70E+04
Lymph node	2.02E+06	1.33E+06	1.03E+06	7.67E+05
Spleen	4.77E+05	3.22E+05	7.65E+04	5.47E+04
Epididymis	3.51E+05	1.38E+05	7.45E+04	5.12E+04
Testes	1.37E+05	5.82E+04	6.94E+04	5.84E+04
Blood	1.30E+06	4.36E+05	1.45E+03	9.38E+02
Bone (femur)	N/A	N/A	1.89E+05	9.60E+04

N/A, not applicable.

vector delivery. While we are currently testing rAAVrh74.MCK.*GALGT2* in a phase 1/2a clinical trial in DMD patients using the ILI method (NCT: 03333590), the studies here provide a framework to amend the *GALGT2* IND to move to systemic i.v. delivery even at very high doses. The current studies are the first to utilize the high doses of AAV that are needed to perfuse all skeletal muscles throughout the body plan, as the previous ILI studies focused only on the lower doses needed for isolated limb delivery.[5,8] Such safety studies, coupled with our recent studies showing prevention of loss of cardiac function in *mdx* mice after i.v. delivery at similar doses,[9] provide a strong rationale for moving forward to systemic i.v. treatment.

We have learned five important things from this study. First, an i.v. dose of 1×10^{14} vg/kg, measured using a linear DNA standard, was sufficient to saturate (1 or more vgs per nucleus) cardiac and skeletal muscles throughout the body plan with AAV, while lower doses also showed significant transduction. While some vgs were lost over time in our toxicity study, which used a dose of 4.3×10^{14} vg/kg, all muscles here also remained at 1 vg per nucleus or greater levels at 3 months post-treatment. The same decrease between 1 and 3 months, however, was not found in muscles treated with rAAVrh74.MCK.*GALGT2* in our dose-response study, suggesting that vector loss over time is not a uniform occurrence. Such variability in muscle transduction over time has also been seen in previous studies of rAAVrh74, where some muscles show a drop in vgs over the course of 3 months while others do not.[6,20] Second, a dose of 4.3×10^{14} vg/kg was sufficient to stimulate *GALGT2*-induced glycosylation in most heart and skeletal muscle cells, while again, lower doses also showed significant glycosylation. The caveat here is that *GALGT2*-induced glycosylation occurred more slowly than induction of *GALGT2* gene expression, which is maximal by 1 month post-treatment[2]. This is perhaps not surprising, as *GALGT2* overexpression primarily induces the glycosylation of α-dystroglycan in skeletal muscle, a membrane protein[12] that can show very slow membrane turnover. Third, *GALGT2*-induced muscle glycosylation studies in mice may underestimate glycosylation in human muscle. The GALGT2 enzyme glycosylates glycans containing a terminal sialic acid,[23,28] and humans do not express the Neu5Gc form of sialic acid due to the presence of an inactivating deletion in the human *CMAH* gene.[27] Sub-saturating doses of rAAVrh74.MCK.*GALGT2* and rAAVrh74.MHCK7.*GALGT2* induced greater glycosylation in *Cmah*-deficient mouse muscles than in *Cmah*-expressing wild-type mouse muscles. Moreover, recombinant human GALGT2 protein bound a known glycan substrate for GALGT2, α2,3-linked sialyl-N-acetyllactosamine, only when Neu5Ac was present and not when Neu5Gc was present. Fourth, delivery of rAAVrh74.MCK.*GALGT2* using a high i.v. dose yielded T cell and antibody responses akin to previous findings using the ILI and IM modes of delivery.[8,20] There was a transient T cell response to two of three rAAVrh74 capsid peptide pools at 4 weeks post-treatment, but these responses were no longer present at 12 weeks. We have previously documented the induction of postnatal death 1 (PD1) and postnatal death ligand 1 (PDL1) expression in IM CD8+ T cells after rAAVrh74.MCK.*GALGT2* treatment in rhesus macaques.[35] Induction of PD1 may help to induce T cell exhaustion after AAV delivery.[36] Fifth, we found no evidence (from analysis of blood cell counts, serum chemistries, or tissue histology) of any treatment-related safety concern (i.e., toxicity). The one possible exception here was that serum ALP activity was significantly elevated after 1 and 3 months of treatment. We could not, however, find elevated ALP activity in any organ or tissue to account for this finding.

Elevated serum ALP, in the absence of elevated AST, ALT, and GGT and in the absence of altered kidney biomarkers (blood urea nitrogen [BUN], creatinine, and total protein) can suggest aberrant bone function—either increased bone growth or increased bone degeneration. However, we saw no elevation in serum calcium or phosphorus beyond normal levels, no change in bone length or weight, and no bone histology to suggest bone toxicity. In theory, increased *GALGT2*-induced muscle glycosylation might directly modify ALP, for example, with the CT glycan, and alter its turnover in serum, but WFA precipitation of serum did not reduce the elevated ALP activity in test-article-treated groups. It is also conceivable that *GALGT2* expression in muscle induces the secretion of a muscle factor that stabilizes ALP in the serum or increases ALP activity. There are case reports of humans with elevated serum ALP where no physical findings were present,[37,38] so elevated serum ALP may not necessarily reflect

the presence of pathology. Indeed, ALP protein and gene therapy treatments—for example, for hypophosphatasia or as a reporter protein—can lead to above normal ALP readings that appear to have no detrimental effects.[39–43]

The highest AAV dose we have used in this study, 4.3×10^{14} vg/kg, is obviously quite large and may not even be a feasible dose for clinical production with current Good Manufacturing Practice (GMP) methodologies. There are, however, three reasons why dosing rAAVrh74.MCK.*GALGT2* in wild-type mice may yield an overly conservative estimate of the doses needed in DMD patients. First, the human GALGT2 enzyme shows more activity in mice with a humanized sialoglycome than it does in normal mice. As all humans lack a functional *CMAH* gene,[27] the increased glycosylation seen in $Cmah^{-/-}$ mice may portend increased potency in human muscles relative to mouse. Second, mice possess a means of capping GALGT2 substrates with glycans that are not even sialic acids; for example, αGal, which, again, differs from human muscle.[44] We show here that human GALGT2 cannot bind α1,3-Gal-linked N-acetyllactosamine, which is an αGal-capped version of sialyl-N-acetyllactosamine (which GALGT2 does bind). Third, the kinetics of *GALGT2*-induced glycosylation is slow in C57BL/6J mice, but it may be faster in DMD muscle, where protein turnover of GALGT2 substrates like dystroglycan likely occurs more quickly due to the absence of dystrophin. The biodistribution study at the 12-week time point showed >1 vg per nucleus of rAAVrh74.MCK.*GALGT2* in the heart and in several skeletal muscles at a dose of 4.8×10^{13} vg/kg, which is about 10 times lower than the highest dose we used, but these muscles did not show a corresponding saturation in *GALGT2*-dependent glycosylation. Similarly, all muscles studied showed 1 or more vgs per nucleus of AAV at a dose of 1.4×10^{14} vg/kg, but again, with the exception of heart, none of these muscles were saturated for glycosylation. In dystrophic muscle, where proteins in the sarcolemmal membrane are being turned over more quickly, the newly glycosylated proteins may be able to better saturate the muscle membrane.

Previous studies have shown that GALGT2 can protect mdx mouse muscles even if only about 15%–20% of the muscle is glycosylated.[5] If one takes glycosylation in wild-type mice as the measure to define the minimally effective dose (MED), then one would say 1×10^{14} vg/kg is the MED, as this dose allowed for 15%–20% glycosylation in all muscles studied. If, however, one assumes that glycosylation in wild-type mice underestimates GALGT2 activity in DMD muscles for the aforementioned listed reasons, one might then use AAV vg transduction in 20% of the musculature to define the MED (or transduction with at least 3.3×10^4 vg/μg genomic DNA). In that case, the MED would be 4.8×10^{13} vg/kg, the dose required to achieve 20% transduction of all muscle nuclei in all muscles tested at the 3-month time point. This dose of 4.8×10^{13} vg/kg (1.3×10^{14} vg/kg, if assayed using a supercoiled DNA standard) is likely just below the highest dose currently being tested in the DMD (NCT: 03375164) and SMA (NCT: 02122952) clinical trials, which is 2×10^{14} vg/kg. Regardless, the use of doses as high as 4.3×10^{14} vg/kg (linear) in the current studies suggest that there may be a very high safety window for dosing in patients.

In conclusion, we have identified doses of rAAVrh74.MCK.*GALGT2* that can accomplish high vector transduction and muscle glycosylation in heart and skeletal muscles with minimal or no microscopic organ toxicity and only expected immunological responses. Such studies support movement to systemic i.v. delivery of rAAVrh74.MCK.*GALGT2* in muscular dystrophy patients.

MATERIALS AND METHODS

Animals

All animals were used in accordance with protocols approved in advance by the Institutional Animal Care and Use Committee at The Research Institute at Nationwide Children's Hospital and following guidelines in the Guide for the Care and Use of Laboratory Animals and the ARRIVE guidelines of NIH. C57BL/6J mice were purchased from The Jackson Laboratory (Bar Harbor, ME, USA). $Cmah^{-/-}$ mice were a generous gift from Ajit Varki (University of California, San Diego). Mice were group housed (maximum, 4 adults per cage) in IVC micro-isolator cages and provided with pelleted chow and tap water (purified through reverse osmosis and UV disinfection) *ad libitum*. Environmental conditions were maintained at 72°F (±2°F), with humidity controlled between 30% and 70% on a 12-h:12-h light-dark cycle. Only male mice were used in this study, as DMD is an X-linked disease occurring almost entirely in boys.[21,22]

Recombinant AAV Production

rAAVrh74.MCK.*GALGT2* and rAAVrh74.MHCK7.*GALGT2* were made using the triple transfection method in HEK293 cells.[45] All transgenes were human cDNA sequences. AAV was purified using iodixanol density separation and anion exchange chromatography as previously described.[45,46]

i.v. AAV Delivery

Mice were placed in a mouse tube restrainer (Braintree Scientific; Braintree, MA, USA) with the tail outside the tube. The injected region was prepped with povidone-iodine and 70% ethanol, after which AAV vector or AAV buffer was injected into the tail vein, usually in a volume of 200 μL and not exceeding a volume of 250 μL. To deliver the (linear) dose of 4.3×10^{14} vg/kg, three injections were required, which were each spaced 2–4 h apart and given on the same day. Titers for i.v. injections were measured using a linear DNA standard. Injected mice exhibited no abnormal clinical signs following any of the injections.

IM AAV Delivery

IM injections were given in the tibialis anterior muscle of wild-type (C57BL/6J) or $Cmah^{-/-}$ mice by direct injection in a volume of 25 μL, with control mice given AAV buffer alone in an identical volume. Doses of rAAVrh74.MCK.*GALGT2* or rAAVrh74.MHCK7.*GALGT2* given were in a total of 3.5×10^9 vg, 3.5×10^{10} vg, or 1.8×10^{11} vg. Titers for IM injections were measured using a linear

DNA standard. Injected mice exhibited no abnormal clinical signs following any of the injections.

Staining for *GALGT2*-Induced Glycosylation in Heart and Skeletal Muscle

WFA staining was used to identify GALGT2 overexpression in skeletal myofibers or cardiomyocytes. Heart and skeletal muscle tissue sections were cut at 10 μm on a cryostat and mounted on slides. Tissue sections were blocked in PBS with 10% donkey serum for 1 h, followed by incubation with anti-laminin α2 antibody (rat monoclonal antibody [mAb] 4H8-2, Sigma) for 1 h at room temperature. Sections were then washed and incubated for 1 h with WFA-fluorescein isothiocyanate (FITC) (EY Laboratories) and Cy3-conjugated donkey anti-rat immunoglobulin G (IgG; Jackson ImmunoResearch Laboratories) at room temperature. After washing, slides were mounted in ProLong Gold anti-fade mounting medium (Molecular Probes) and imaged using a Zeiss Axioskop 2 epifluorescence microscope with the appropriate fluorescence filters, with images captured on a Zeiss AxioCam MRC5 camera. All WFA-stained images were time matched for exposure to allow for comparisons among images.

Toxicity and Biodistribution Study Design

Injection and in-life analysis was done independently by the Animal Resources Core at The Abigail Wexner Research Institute at Nationwide Children's Hospital. Wild-type, male, 7-week-old C57BL/6J mice were randomized, sorted into 4 groups of 7 mice each, and allowed to acclimate for at least 5 days prior to injection. At 8 weeks of age, two groups of mice received i.v. injections of 4.3×10^{14} vg/kg rAAVrh74.MCK.*GALGT2* (Research Grade lot TT452-1, measured using a linear DNA standard), and two groups were injected with an equivalent volume of AAV buffer alone (lot 020917DS-02). All mice received three injections, spaced 2–4 h apart, with a volume of no more than 200 μL per injection or less (except one animal that received one 212-μL injection). All mice weighed between 18 and 20 g at the time of injection. Mice were housed in the barrier facility at the Research Institute. Animals were observed once daily for signs of toxicity, including changes to skin, fur, eyes, mucous membranes, respiratory system, circulatory system, autonomic CNS, somatomotor activity, locomotor activity, and behavioral patterns. In addition, there was a once-daily assessment of moribundity and mortality. Body weights were collected weekly. Mice were bled via the facial vein/submandibular vein 1 week prior to necropsy. One control group and one AAV-treated group were euthanized at 4 weeks post-treatment, and one control group and one AAV-treated group were euthanized at 12 weeks post-treatment for collection of blood, serum, and selected organs for further analysis.

Blood Collection, Serum Separation, and Analysis

Whole blood was collected by nicking the submandibular vein 1 week prior to euthanasia for all groups. From this, serum was separated, and certain serum chemistries were analyzed. At euthanasia, mice were anesthetized with ketamine/xylazine, and whole blood was isolated by cardiac puncture after dissection of the sternum, some of which was separated into serum and some of which was harvested in heparinized tubes for whole blood analysis. All blood and serum measures except ELISpot assays and anti-rAAVrh74 serum ELISAs were done by ANTECH GLP (Morrisville, NC, USA).

Histopathology Analysis

Organs were removed and fixed by immersion in neutral-buffered 10% formalin and given to the Biopathology Core at Nationwide Children's Hospital, which performed routine processing, sectioning, and mounting of thin sections on slides, followed by staining with H&E. For the 12-week treatment and control groups, the femur bones were also dissected and fixed by immersion in saline-saturated 10% formalin at room temperature for 24 h but were then decalcified for 5 days at room temperature in Rapid Cal Immuno (BBC Biochemical, Mount Vernon, WA, USA) prior to sending to the Biopathology Core for processing. Slides were evaluated by an American College of Veterinary Pathologists (ACVP) board-certified veterinary pathologist (B.B.) using a tiered, semiquantitative, scoring scheme (i.e., within normal limits or mild, moderate, or marked lesions) and a coded analytical strategy, i.e., analysis made without knowledge of the treatment ("blinded").

ELISA for Antibody Responses to rAAVrh74 Capsid Protein

96-well ELISA plates were coated with 2×10^9 DRP of rAAVrh74 virus or were not coated as controls. Serum was added at 2-fold dilutions, beginning at a 1:100 dilution, to virus-coated and control wells for 1 h. Plates were then washed with PBS and incubated with anti-mouse IgG linked to horseradish peroxidase (HRP), washed, and developed and read as previously described.[6] Endpoint titer was calculated based on the reciprocal value of the last serum dilution to yield a signal 2-fold above background. A positive control serum from a mouse previously immunized with rAAVrh74.MCK.*GALGT2* and a negative control from a mouse never given AAV were used in assays for all samples.

γ–Interferon ELISpot Assay

Splenocytes were collected from the 4-week and 12-week treatment and control groups as previously described.[6] Isolated cells were counted, and a solution of 10^6 splenocytes per milliliter was used to seed the wells of a 96-well polyvinylidene fluoride (PVDF)-coated filter plate (Millipore, Burlington, MA, USA) with 2×10^5 cells per well. Three pools of overlapping peptides comprising the entire sequence of the rAAVrh74 capsid protein, or two pools of peptides comprising the entire sequence of the GALGT2 protein, all 18 aa in length, were added at 0.2 μg to cells to assess T cell responses. 2 μg concanavalin A (ConA) was used as a positive control, and vehicle alone (DMSO) was used as a negative control. All assays were done in triplicate. After 36–48 h of incubation in a sterile cell incubator at 37°C with 5% CO_2, cells were washed and developed for mouse γ-interferon (U-Cytech). Positive cells were counted on a plate reader as previously described.[6,20]

Quantitative PCR

TaqMan quantitative PCR (qPCR) was used to quantify the number of AAV vgs from genomic DNA extracted from snap-frozen, unfixed

organ and muscle shavings and whole blood samples. All skeletal and cardiac muscles and all non-muscle organs studied for dose-response studies and for toxicity studies were analyzed. The QIAGEN DNeasy Blood and Tissue Kit was used to extract genomic DNA following the manufacturer's protocols. 100 ng genomic DNA was assayed by qPCR using primers specific to the AAV vector genome: forward, 5′-CCTCAGTGGATGTTGCCTTTA-3′; probe, 5′-/56-FAM/AAA GCTGCG/ZEN/GAATTGTACCCGC/3lABVkFQ-3′; and reverse, 5′-ATCTTGAGGAGCCACAGAAATC-3′. The pAAV.MCK.*GALGT2* plasmid was cut with Cla1 and purified for use as a linear DNA standard. This standard was measured between 50 and 5 million copies in logarithmic increments to generate a linear calibration, for which the Pearson correlation coefficient always equaled or exceeded 0.98. qPCR measures were done on an Applied Biosystems 7500 Sequence Detection System. Each sample was run in triplicate, and the values were averaged. Some samples were spiked with 100 copies of pAAV.MCK.*GALGT2* standard and measured to ensure no quenching of signal by genomic DNA or by contaminants from the extraction procedure.

Measurement of relative transcription levels

Measures of human (*GALGT2*) and mouse (*Galgt2*) mRNA levels were done using the $2^{-\Delta\Delta CT}$ method with 18S rRNA as a reference standard, as previously described.[26,47]

ELISA Assays of ALP Protein and Activity

To measure serum ALP activity, 10 μL serum was diluted into 190 μL assay mixture and developed using the QuantiChrom ALP Assay Kit (BioAssay Systems, Hayward, CA, USA) following the manufacturer's instructions. For some measures, 15 μL serum was first precipitated with 10 μL WFA bound to agarose (EY Laboratories, San Mateo, CA, USA). After 1 h of incubation, samples were centrifuged at 3,000 × *g* for 3 min, and unbound supernatant was then compared to serum without WFA precipitation using the QuantiChrom ALP Assay Kit (BioAssay Systems, Hayward, CA, USA) following the manufacturer's instructions. To measure ALP activity in tissues, tissue lysates were made at 4°C using lysis buffer containing 1% NP-40 in Tris-buffered saline (pH 7.4), with complete protease inhibitors (Sigma, St. Louis, MO, USA). Protein concentrations were determined using the Micro BCA Protein Assay Kit (Thermo Scientific Pierce, Rockford, IL, USA). A constant amount of 50 μg protein was measured using the QuantiChrom ALP Assay Kit (BioAssay Systems, Hayward, CA, USA) following the manufacturer's instructions. Serum ALP protein levels were measured using the Mouse ALP ELISA Kit (Biomatik, Cambridge, ON, Canada) following the manufacturer's instructions.

Binding of PAA-Glycans to Human GALGT2 Protein, Mouse Galgt2 Protein, Recombinant Laminin, or Recombinant Agrin

Polyacrylamide (PAA)-linked glycans, which contained biotin, were obtained from the Consortium for Functional Glycomics (www.functionalglycomics,org) or were purchased from Glycotech (Gaithersburg, MD, USA). PAA-biotin conjugates used were: Neu5Acα2,3Galβ1,4GlcNAcβ-SpNH-PAA (3′SNL 5Ac), Neu5Gcα2,3Galβ1,4GlcNAcβ-SpNH-PAA (3′SNL 5Gc), Neu5Acα2,3[GalNAcβ1,4]Galβ1,4GlcNAcβ-SpNH-PAA (CT 5Ac), Neu5Acα2,6Galβ1,4GlcNAcβ-SpNH-PAA (6′SNL 5Ac), Neu5Gcα2,6Galβ1,4GlcNAcβ-SpNH-PAA (6′SNL 5Gc), Galβ1,4GlcNAcβ-SpNH-PAA (NL), Galβ1,4GlcNAcβ1,3Galβ1,4GlcNAcβ-SpNH-PAA (diNL), and Galα1,3Galβ1,4GlcNAcβ-SpNH-PAA (GalNL), where Neu5Ac is N-acetyl-neuraminic acid, Neu5Gc is N-glycolyl-neuraminic acid, Gal is galactose, GlcNAc is N-acetylglucosamine, and GalNAc is N-acetylgalactosamine. Soluble secreted luminal domains of human GALGT2 protein and mouse Galgt2 protein were made with an N-terminal FLAG (DYKDDDDK) epitope tag. cDNAs encoding human *GALGT2* and mouse *Galgt2* were transfected into HEK293 cells, and protein was collected from the supernatant and purified using anti-FLAG (M2 antibody) immunopurification, as previously described.[47] Likewise, recombinant forms of the G1–G5 domains of laminin α2, α4, or α5, or the G2–G3 domains of the muscle (z0) or neural (z8) splice forms of agrin, all containing an N-terminal FLAG epitope tag, were purified as previously described.[47] Briefly, the recombinant purified protein (500 ng) was immobilized on ELISA (96-well) plates in sodium bicarbonate buffer (50 mM [pH 9.5]) overnight at 4°C. After washing in Tris-buffered saline (TBS), polyacrylamide (PAA) and biotin-linked glycans, conjugated via an Sp (-$CH_2Ch_2N_3$) spacer where the molecular weight was 30 kDa (20% glycan, 5% biotin), were added at 1 μg/mL for 2 h at room temperature, washed, and incubated with HRP-conjugated streptavidin (1:1,000) for 1 h. After further washing, plates were developed in SIGMAFAST OPD (o-phenylenediamine dihydrochloride), a peroxidase substrate, and read at 450 nm on a SpectraMax plate reader. Plates were read multiple times (at 1, 5, 10, 20, 30, 40, 50, and 60 min) until maximal plate signal approached 1.0. Binding of all glycans was then normalized to maximal binding at 1. All data points used represent averages of triplicate measures for each condition.

SUPPLEMENTAL INFORMATION

Supplemental Information can be found online at https://doi.org/10.1016/j.omtm.2019.10.005.

AUTHOR CONTRIBUTIONS

D.A.Z. and P.T.M. were primarily responsible for writing the manuscript, with editorial input from all other authors. D.A.Z., R.X., and Y.J. performed dose-response glycosylation, biodistribution, and gene expression studies, with assistance in quantification of measures by S.H. D.A.Z. performed anti-rAAVrh74 serum ELISA studies as well as organ ALP activity assays and serum ALP dose-response assays. R.X. performed all ELISpot assays on splenocytes and dosed all mice for the dose-response study. A.A., C.M., and H.P. dosed mice for the toxicity study and performed all mouse in-life observational studies and necropsy studies. G.S. performed dose-response IM studies comparing wild-type and *Cmah*$^{-/-}$ mice. J.H.Y. performed PAA-glycan binding studies to recombinant proteins. B.B. performed all tissue histopathology analyses, and P.T.M. was responsible for experimental design.

CONFLICTS OF INTEREST

P.T.M. receives licensing payments for rAAVrh74.MCK.*GALGT2* from Sarepta Therapeutics. The other authors declare no competing interests.

ACKNOWLEDGMENTS

This work was funded by grants from Parent Project Muscular Dystrophy and NIH (R01 AR049722 and P50 AR070604) to P.T.M. Data shown in Figures 5A and 5B were supported by DOD grant W81XWH-12-1-0416 to P.T.M. We would like to thank Megan Cramer and Haley Guggenheim for technical support and Ajit Varki (UC San Diego) for the gift of *Cmah*$^{-/-}$ mice.

REFERENCES

1. Nguyen, H.H., Jayasinha, V., Xia, B., Hoyte, K., and Martin, P.T. (2002). Overexpression of the cytotoxic T cell GalNAc transferase in skeletal muscle inhibits muscular dystrophy in mdx mice. Proc. Natl. Acad. Sci. USA *99*, 5616–5621.

2. Xu, R., Chandrasekharan, K., Yoon, J.H., Camboni, M., and Martin, P.T. (2007). Overexpression of the cytotoxic T cell (CT) carbohydrate inhibits muscular dystrophy in the dyW mouse model of congenital muscular dystrophy 1A. Am. J. Pathol. *171*, 181–199.

3. Xu, R., Camboni, M., and Martin, P.T. (2007). Postnatal overexpression of the CT GalNAc transferase inhibits muscular dystrophy in mdx mice without altering muscle growth or neuromuscular development: evidence for a utrophin-independent mechanism. Neuromuscul. Disord. *17*, 209–220.

4. Xu, R., DeVries, S., Camboni, M., and Martin, P.T. (2009). Overexpression of Galgt2 reduces dystrophic pathology in the skeletal muscles of alpha sarcoglycan-deficient mice. Am. J. Pathol. *175*, 235–247.

5. Martin, P.T., Xu, R., Rodino-Klapac, L.R., Oglesbay, E., Camboni, M., Montgomery, C.L., Shontz, K., Chicoine, L.G., Clark, K.R., Sahenk, Z., et al. (2009). Overexpression of *Galgt2* in skeletal muscle prevents injury resulting from eccentric contractions in both mdx and wild-type mice. Am. J. Physiol. Cell Physiol. *296*, C476–C488.

6. Chicoine, L.G., Montgomery, C.L., Bremer, W.G., Shontz, K.M., Griffin, D.A., Heller, K.N., Lewis, S., Malik, V., Grose, W.E., Shilling, C.J., et al. (2014). Plasmapheresis eliminates the negative impact of AAV antibodies on microdystrophin gene expression following vascular delivery. Mol. Ther. *22*, 338–347.

7. Thomas, P.J., Xu, R., and Martin, P.T. (2016). B4GALNT2 (GALGT2) gene therapy reduces skeletal muscle pathology in the FKRP P448L mouse model of limb girdle muscular dystrophy 2I. Am. J. Pathol. *186*, 2429–2448.

8. Xu, R., Jia, Y., Zygmunt, D.A., Cramer, M.L., Crowe, K.E., Shao, G., Maki, A.E., Guggenheim, H.N., Hood, B.C., Griffin, D.A., et al. (2018). An isolated limb infusion method allows for broad distribution of rAAVrh74.MCK.*GALGT2* to leg skeletal muscles in the rhesus macaque. Mol. Ther. Methods Clin. Dev. *10*, 89–104.

9. Xu, R., Jia, Y., Zygmunt, D.A., and Martin, P.T. (2019). rAAVrh74.MCK.GALGT2 protects against loss of hemodynamic function in the aging *mdx* mouse heart. Mol. Ther. *27*, 636–649.

10. Martin, P.T., Scott, L.J., Porter, B.E., and Sanes, J.R. (1999). Distinct structures and functions of related pre- and postsynaptic carbohydrates at the mammalian neuromuscular junction. Mol. Cell. Neurosci. *13*, 105–118.

11. Hoyte, K., Kang, C., and Martin, P.T. (2002). Definition of pre- and postsynaptic forms of the CT carbohydrate antigen at the neuromuscular junction: ubiquitous expression of the CT antigens and the CT GalNAc transferase in mouse tissues. Brain Res. Mol. Brain Res. *109*, 146–160.

12. Xu, R., Singhal, N., Serinagaoglu, Y., Chandrasekharan, K., Joshi, M., Bauer, J.A., Janssen, P.M., and Martin, P.T. (2015). Deletion of Galgt2 (B4Galnt2) reduces muscle growth in response to acute injury and increases muscle inflammation and pathology in dystrophin-deficient mice. Am. J. Pathol. *185*, 2668–2684.

13. Ohlendieck, K., Ervasti, J.M., Matsumura, K., Kahl, S.D., Leveille, C.J., and Campbell, K.P. (1991). Dystrophin-related protein is localized to neuromuscular junctions of adult skeletal muscle. Neuron *7*, 499–508.

14. Hoch, W., Ferns, M., Campanelli, J.T., Hall, Z.W., and Scheller, R.H. (1993). Developmental regulation of highly active alternatively spliced forms of agrin. Neuron *11*, 479–490.

15. Patton, B.L., Miner, J.H., Chiu, A.Y., and Sanes, J.R. (1997). Distribution and function of laminins in the neuromuscular system of developing, adult, and mutant mice. J. Cell Biol. *139*, 1507–1521.

16. Chiu, A.Y., and Sanes, J.R. (1984). Development of basal lamina in synaptic and extrasynaptic portions of embryonic rat muscle. Dev. Biol. *103*, 456–467.

17. Rezniczek, G.A., Konieczny, P., Nikolic, B., Reipert, S., Schneller, D., Abrahamsberg, C., Davies, K.E., Winder, S.J., and Wiche, G. (2007). Plectin 1f scaffolding at the sarcolemma of dystrophic (*mdx*) muscle fibers through multiple interactions with beta-dystroglycan. J. Cell Biol. *176*, 965–977.

18. Rupp, F., Payan, D.G., Magill-Solc, C., Cowan, D.M., and Scheller, R.H. (1991). Structure and expression of a rat agrin. Neuron *6*, 811–823.

19. Xia, B., Hoyte, K., Kammesheidt, A., Deerinck, T., Ellisman, M., and Martin, P.T. (2002). Overexpression of the CT GalNAc transferase in skeletal muscle alters myofiber growth, neuromuscular structure, and laminin expression. Dev. Biol. *242*, 58–73.

20. Chicoine, L.G., Rodino-Klapac, L.R., Shao, G., Xu, R., Bremer, W.G., Camboni, M., Golden, B., Montgomery, C.L., Shontz, K., Heller, K.N., et al. (2014). Vascular delivery of rAAVrh74.MCK.GALGT2 to the gastrocnemius muscle of the rhesus macaque stimulates the expression of dystrophin and laminin α2 surrogates. Mol. Ther. *22*, 713–724.

21. Hoffman, E.P., Brown, R.H., Jr., and Kunkel, L.M. (1987). Dystrophin: the protein product of the Duchenne muscular dystrophy locus. Cell *51*, 919–928.

22. Koenig, M., Hoffman, E.P., Bertelson, C.J., Monaco, A.P., Feener, C., and Kunkel, L.M. (1987). Complete cloning of the Duchenne muscular dystrophy (DMD) cDNA and preliminary genomic organization of the DMD gene in normal and affected individuals. Cell *50*, 509–517.

23. Smith, P.L., and Lowe, J.B. (1994). Molecular cloning of a murine N-acetylgalactosamine transferase cDNA that determines expression of the T lymphocyte-specific CT oligosaccharide differentiation antigen. J. Biol. Chem. *269*, 15162–15171.

24. Shaw, L., Schneckenburger, P., Carlsen, J., Christiansen, K., and Schauer, R. (1992). Mouse liver cytidine-5′-monophosphate-N-acetylneuraminic acid hydroxylase. Catalytic function and regulation. Eur. J. Biochem. *206*, 269–277.

25. Kawano, T., Koyama, S., Takematsu, H., Kozutsumi, Y., Kawasaki, H., Kawashima, S., Kawasaki, T., and Suzuki, A. (1995). Molecular cloning of cytidine monophospho-N-acetylneuraminic acid hydroxylase. Regulation of species- and tissue-specific expression of N-glycolylneuraminic acid. J. Biol. Chem. *270*, 16458–16463.

26. Chandrasekharan, K., Yoon, J.H., Xu, Y., deVries, S., Camboni, M., Janssen, P.M., Varki, A., and Martin, P.T. (2010). A human-specific deletion in mouse *Cmah* increases disease severity in the mdx model of Duchenne muscular dystrophy. Sci. Transl. Med. *2*, 42ra54.

27. Chou, H.H., Takematsu, H., Diaz, S., Iber, J., Nickerson, E., Wright, K.L., Muchmore, E.A., Nelson, D.L., Warren, S.T., and Varki, A. (1998). A mutation in human CMP-sialic acid hydroxylase occurred after the *Homo-Pan* divergence. Proc. Natl. Acad. Sci. USA *95*, 11751–11756.

28. Montiel, M.D., Krzewinski-Recchi, M.A., Delannoy, P., and Harduin-Lepers, A. (2003). Molecular cloning, gene organization and expression of the human UDP-GalNAc:Neu5Acalpha2-3Galbeta-R beta1,4-N-acetylgalactosaminyltransferase responsible for the biosynthesis of the blood group Sda/Cad antigen: evidence for an unusual extended cytoplasmic domain. Biochem. J. *373*, 369–379.

29. Varki, A. (2010). Colloquium paper: uniquely human evolution of sialic acid genetics and biology. Proc. Natl. Acad. Sci. USA *107* (*Suppl 2*), 8939–8946.

30. Varki, A. (2009). Multiple changes in sialic acid biology during human evolution. Glycoconj. J. *26*, 231–245.

31. Salva, M.Z., Himeda, C.L., Tai, P.W., Nishiuchi, E., Gregorevic, P., Allen, J.M., Finn, E.E., Nguyen, Q.G., Blankinship, M.J., Meuse, L., et al. (2007). Design of tissue-specific regulatory cassettes for high-level rAAV-mediated expression in skeletal and cardiac muscle. Mol. Ther. *15*, 320–329.

32. Dall'Olio, F., Malagolini, N., Chiricolo, M., Trinchera, M., and Harduin-Lepers, A. (2014). The expanding roles of the Sd(a)/Cad carbohydrate antigen and its cognate glycosyltransferase B4GALNT2. Biochim. Biophys. Acta *1840*, 443–453.

33. Rosas, L.E., Grieves, J.L., Zaraspe, K., La Perle, K.M., Fu, H., and McCarty, D.M. (2012). Patterns of scAAV vector insertion associated with oncogenic events in a mouse model for genotoxicity. Mol. Ther. *20*, 2098–2110.

34. Nelson, C.E., Wu, Y., Gemberling, M.P., Oliver, M.L., Waller, M.A., Bohning, J.D., Robinson-Hamm, J.N., Bulaklak, K., Castellanos Rivera, R.M., Collier, J.H., et al. (2019). Long-term evaluation of AAV-CRISPR genome editing for Duchenne muscular dystrophy. Nat. Med. *25*, 427–432.

35. Cramer, M.L., Shao, G., Rodino-Klapac, L.R., Chicoine, L.G., and Martin, P.T. (2017). Induction of T-cell infiltration and programmed death ligand 2 expression by adeno-associated virus in rhesus macaque skeletal muscle and modulation by prednisone. Hum. Gene Ther. *28*, 493–509.

36. Velazquez, V.M., Bowen, D.G., and Walker, C.M. (2009). Silencing of T lymphocytes by antigen-driven programmed death in recombinant adeno-associated virus vector-mediated gene therapy. Blood *113*, 538–545.

37. Lucas, A., Brooke, O.G., Baker, B.A., Bishop, N., and Morley, R. (1989). High alkaline phosphatase activity and growth in preterm neonates. Arch. Dis. Child. *64*, 902–909.

38. Verma, J., and Gorard, D.A. (2012). Persistently elevated alkaline phosphatase. BMJ Case Rep. *2012*, bcr2012006768.

39. Pickkers, P., Mehta, R.L., Murray, P.T., Joannidis, M., Molitoris, B.A., Kellum, J.A., Bachler, M., Hoste, E.A.J., Hoiting, O., Krell, K., et al.; STOP-AKI Investigators (2018). Effect of human recombinant alkaline phosphatase on 7-day creatinine clearance in patients with sepsis-associated acute kidney injury: a randomized clinical trial. JAMA *320*, 1998–2009.

40. Nakamura-Takahashi, A., Miyake, K., Watanabe, A., Hirai, Y., Iijima, O., Miyake, N., Adachi, K., Nitahara-Kasahara, Y., Kinoshita, H., Noguchi, T., et al. (2016). Treatment of hypophosphatasia by muscle-directed expression of bone-targeted alkaline phosphatase via self-complementary AAV8 vector. Mol. Ther. Methods Clin. Dev. *3*, 15059.

41. Matsumoto, T., Miyake, K., Yamamoto, S., Orimo, H., Miyake, N., Odagaki, Y., Adachi, K., Iijima, O., Narisawa, S., Millán, J.L., et al. (2011). Rescue of severe infantile hypophosphatasia mice by AAV-mediated sustained expression of soluble alkaline phosphatase. Hum. Gene Ther. *22*, 1355–1364.

42. Qiao, C., Zhang, W., Yuan, Z., Shin, J.H., Li, J., Jayandharan, G.R., Zhong, L., Srivastava, A., Xiao, X., and Duan, D. (2010). Adeno-associated virus serotype 6 capsid tyrosine-to-phenylalanine mutations improve gene transfer to skeletal muscle. Hum. Gene Ther. *21*, 1343–1348.

43. Bostick, B., Ghosh, A., Yue, Y., Long, C., and Duan, D. (2007). Systemic AAV-9 transduction in mice is influenced by animal age but not by the route of administration. Gene Ther. *14*, 1605–1609.

44. Galili, U. (2013). Anti-Gal: an abundant human natural antibody of multiple pathogeneses and clinical benefits. Immunology *140*, 1–11.

45. Xiao, X., Li, J., and Samulski, R.J. (1998). Production of high-titer recombinant adeno-associated virus vectors in the absence of helper adenovirus. J. Virol. *72*, 2224–2232.

46. Clark, K.R., Liu, X., McGrath, J.P., and Johnson, P.R. (1999). Highly purified recombinant adeno-associated virus vectors are biologically active and free of detectable helper and wild-type viruses. Hum. Gene Ther. *10*, 1031–1039.

47. Yoon, J.H., Chandrasekharan, K., Xu, R., Glass, M., Singhal, N., and Martin, P.T. (2009). The synaptic CT carbohydrate modulates binding and expression of extracellular matrix proteins in skeletal muscle: Partial dependence on utrophin. Mol. Cell. Neurosci. *41*, 448–463.